CO oxidation from syngas (CO and H₂) using nanoporous Pt/Al₂O₃ catalyst

Jong-Soo Bae*, Joo-Won Park*, Jae-Ho Kim**, Jae-Goo Lee**, Younghun Kim*, and Choon Han*,†

*Department of Chemical Engineering, Kwangwoon University, Seoul 139-701, Korea
**Gasification Research Center, Korea Institute of Energy Research, Daejeon 305-343, Korea

Abstract−The concept of "waste-to-wealth" is spreading awareness to prevent global warming and recycle the restrictive resources. To contribute towards sustainable development, hydrogen energy is obtained from syngas (CO and H₂) generated from waste gasification, followed by CO oxidation and CO₂ removal. In H₂ generation, it is key to produce more purified H₂ from syngas using heterogeneous catalysts. In this respect, we prepared Pt/Al₂O₃ catalyst with nanoporous structure using precipitation method, and compared its catalytic activity with commercial alumina (Degussa). Based on the results of XRD and TEM, it was found that metal particles did not aggregate on the alumina surface and showed high dispersion. Optimum condition for CO conversion was 1.5 wt% Pt loaded on Al₂O₃ support, and pure hydrogen was obtained after removal of CO₂ gas.

Key words: CO Oxidation, Pt/Al₂O₃, Nanoporous Alumina, Hydrogen Energy

INTRODUCTION

Almost all the energies we use depend on fossil fuel. While fossil fuels obtained from underground resources have some advantages like shipping and using easily, they have serious drawbacks, such as environmental problems and limited amounts. Therefore, studies for the development of alternative energy have been reported to prevent environmental pollution and to contribute towards sustainable development [1-3]. Natural energy resources including solar and wind have already been used in practical fields as alternative energies [4,5]. Recently, studies about hydrogen generation to replace fossil fuel have been lively reported [6,7]. Herein, it is key to produce hydrogen energy without environmental pollution from unlimited resources, such as syngas (CO, CO₂, H₂, etc.) generated from waste gasification. This concept could be called as "waste-to-wealth", which is spreading awareness to prevent global warming and recycle the restrictive resources.

Hydrogen could be generated from several well-known reactions: methane reforming ($CH_4+H_2O \rightarrow CO+3H_2$) [8], water gas shift ($CO+H_2O \rightarrow CO_2+H_2$) [9], partial oxidation ($CH_4+1/2O_2 \rightarrow CO+2H_2$) [10], and carbon dioxide reforming ($CH_4+CO_2 \rightarrow 2CO+2H_2$) [11]. The final resultant in those reactions is the mixture of CO, CO₂, and H₂, so post-treatment like H₂ separation should be considered to obtain pure H₂. In addition, to improve the selectivity of H₂ in the syngas, some progressing methods have been developed: PSA (pressure swing adsorption) [12], membrane separation [13], and catalytic conversion using heterogeneous catalyst. Among these reactions, metal catalyst is recommended due to easy preparation, simple process, and high physical/chemical stability.

CO can be removed by preferential oxidation (PROX) using Pt. Based on the Langmuir-Hinshelwood model, which is different from the kinetics for $CO+1/2O_2 \rightarrow CO_2$ [14], CO oxidation using M/Al₂O₃

catalyst has progressed as follows:

$$\begin{aligned} CO+\text{free site} &\rightarrow CO_{ad} \\ O_2+\text{free site} &\rightarrow 2O_{ad} \\ CO_{ad}+O_{ad}+H_2 &\rightarrow CO_2+H_2 \end{aligned} \tag{1}$$

H₂ selectivity was improved by adsorbing CO₂ using alkali carbonates as adsorbents which can comparatively adsorb CO₂ at low temperature [15].

$$CO_2+X_2CO_3+H_2O+H_2 \rightarrow 2XHCO_3+H_2 \text{ (X=alkali metals)} \tag{2}$$
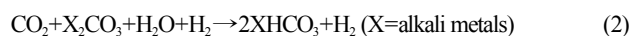
In this study, to convert CO generated from waste gasification into CO₂, Pt/Al₂O₃ catalyst with nanoporous structure was prepared and tested under several conditions. The activities of the catalyst prepared were compared with commercial alumina (Degussa).

EXPERIMENTAL

1. Preparation and Characterization of Nanoporous Pt/Al₂O₃ Catalysts

As a metal oxide support, nanoporous alumina was prepared by templating method, which was previously reported [16]. Aluminum sec-butoxide and lauric acid were used as precursor and template, respectively. Dried white powder was calcined at 550 °C for 5 hr for removal of surfactant. Catalytic active metal (Pt) was immobilized via precipitation method, and then 0.5 to 1.5 wt% Pt could be loaded on the alumina support.

Pore size, surface area and pore volume of all samples were analyzed with ASAP-2010 (Micromeritics). Crystallinity of catalysts was measured with X-ray diffraction (D5005, Bruker). The metal dispersion and pore morphology were confirmed by transmission electron microscopy (LIBRA 120, Carl Zeiss).

2. CO Oxidation Test

CO oxidation was tested in a fixed bed reactor (Fig. 1). Catalyst (300 mg) was loaded on tubular quartz (working tube bore×outer length (mm): 15Ø×200L) using glass membrane filter. MFCs (mass

†To whom correspondence should be addressed.
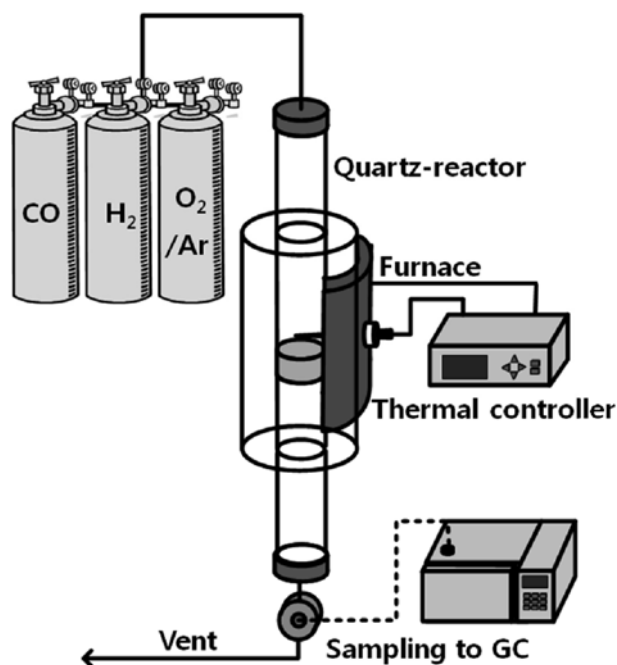E-mail: chan@daisy.kw.ac.kr

Fig. 1. Schematic diagram of CO oxidation system.

flow controller) were installed in each gas cylinder to adjust gas-flow rate. Gas-flow was an equimolar mixture of CO_2, H_2, and O_2/Ar, and total gas rate was fixed to 300 ml/min. At this time, CO concentration of input was 33.3%. The reactor was heated using a furnace, and thermocouple was installed on the catalyst surface. The resultant gas following reaction was periodically sampled at the sampling port using a syringe and analyzed with HP5890 GC (TCD detector, carbosieve s-II column).

RESULTS AND DISCUSSION

1. Characteristics of Nanoporous Pt/Al₂O₃

As shown in Table 1, pore properties of as-made alumina and Pt/Al₂O₃ catalysts with different metal loading were analyzed with N_2 adsorption/desorption test (Fig. 2) and summarized. Alumina support has regular nanopore (5.6 nm) and shows high surface area (above 300 m²/g), which is suitable for application in catalytic supports or adsorbents. As shown in Fig. 2, Degussa alumina showed broad pore size distribution, which was revealed from textural porosity of aggregation of primary particle. This void fraction represented in 0.8-1.0 P/P$_o$ (Fig. 2) caused the bottle-neck phenomenon during
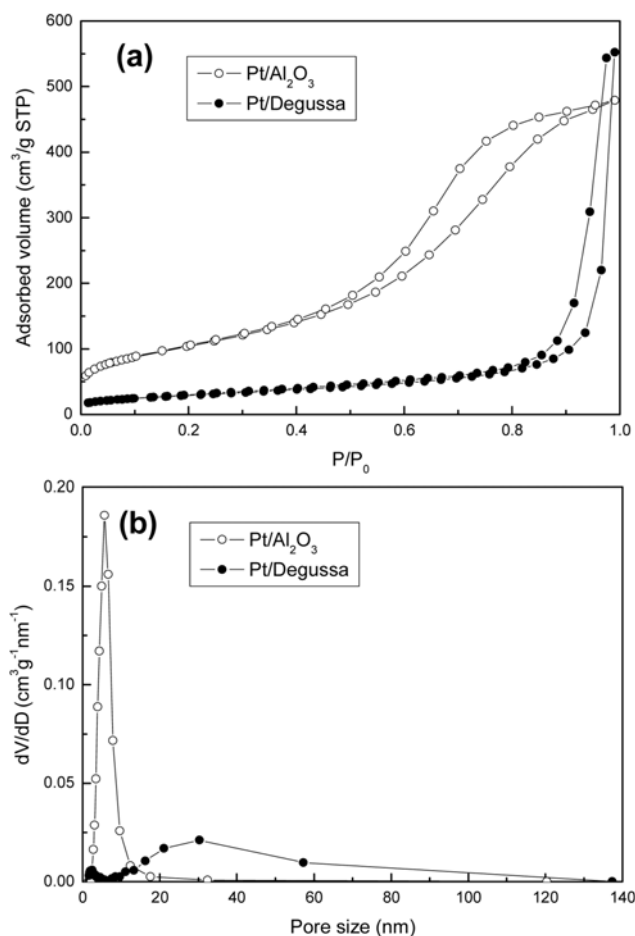

Fig. 2. (a) N₂ adsorption/desorption isotherms and (b) pore size distribution of 1.5 wt% Pt/Al₂O₃ (nanoporous alumina and Degussa).

metal loading and catalytic reaction. Meanwhile, as-made alumina showed framework porosity (0.5-0.8 P/P$_o$ in Fig. 2), which was made by template and helpful to prepare highly dispersed metal catalyst. And as-made alumina showed 3 times larger surface area as compared with Degussa, and then showed higher catalytic activity. As metal loading increased from 0 to 1.5 wt%, surface and pore volume slightly decreased. It is noted that Pt loading was not affected by the physical structure of support.

Metal dispersion was analyzed with TEM and XRD test (Fig. 3 and Fig. 4). Fig. 3 shows TEM images of 1.5 wt% Pt/Al₂O₃. Although the same amount of metal was loaded on different alumina supports (nanoporous alumina and Degussa), Pt/Degussa showed aggregation of Pt particles on the support (Fig. 3(b)). This might be due to the poor nanopore structure of the support compared with as-made alumina. High dispersion of Pt was confirmed by XRD analysis (Fig. 4). When a metal particle is very small, metal peaks decrease and are hidden in the main peaks of the alumina structure. In addition, the characteristic peak position of Pt [(110), (200) and (220)] was overlapped with that of γ-alumina [(222), (400) and (440)], so peak definition for Pt was difficult. As shown in diffraction patterns of Pt/Al₂O₃, diffractions of Pt cannot be distinguished from Pt contents. It should be noted that Pt/Al₂O₃ catalysts prepared by precipitation method showed highly dispersed Pt.

Table 1. Pore properties of supports and catalysts

Samples	wt%	Pore size (nm)	Surface area (m²/g)	Pore volume (cm³/g)
Nanoporous alumina	-	5.63	374.58	0.78
Degussa alumina	-	10.91	118.16	0.28
Pt/Al₂O₃	0.5	5.67	373.54	0.78
	1.0	5.67	370.81	0.77
	1.5	5.67	366.04	0.73
Pt/Degussa	1.5	30.27	104.09	0.86
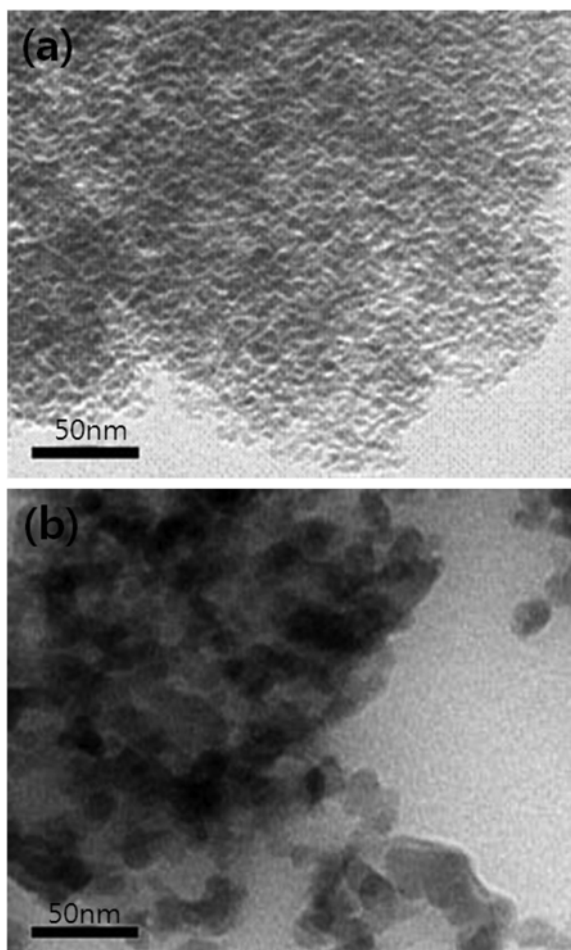
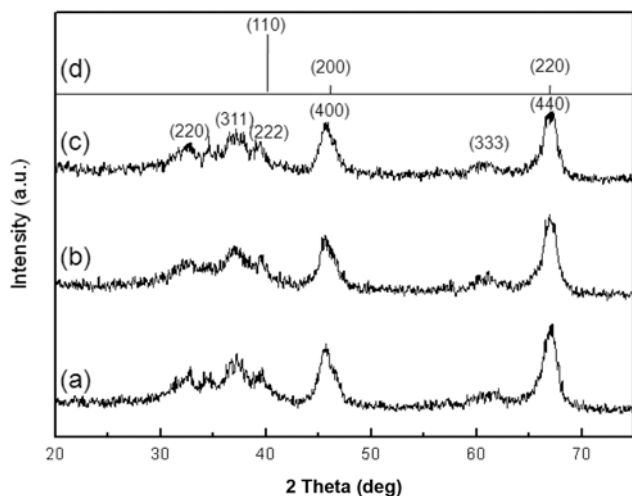Fig. 3. TEM images of (a) as-made nanoporous catalyst and (b) Degussa catalyst.
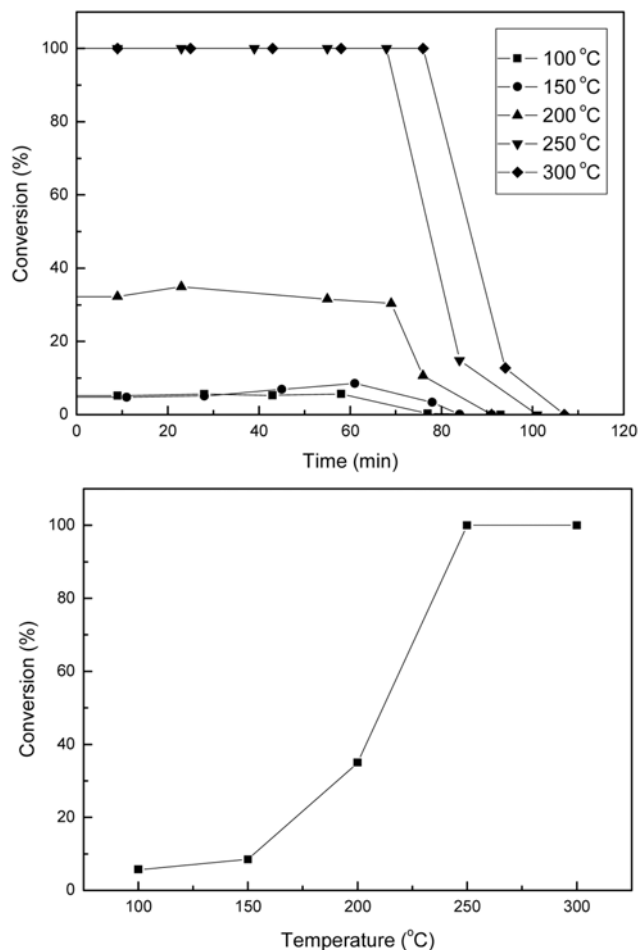

Fig. 5. CO conversion with reaction temperature using 4.0 wt% Pt/Al$_2$O$_3$ catalyst.

CO conversion for reaction temperature was performed in a fixed bed reactor using 4.0 wt% Pt/Al$_2$O$_3$ catalyst to predict the highest active temperature region (Fig. 5). CO conversion was calculated using Eq. (3). Where, C$_{CO_i}$ and C$_{CO_o}$ are the CO concentrations of inlet gas and exit gas, respectively.

$$\text{CO conversion } (\%) = \left(1 - \frac{C_{CO_o}}{C_{CO_i}}\right) \times 100 \qquad (3)$$

As shown in Fig. 5, CO conversions to CO$_2$ reached to 5.7, 8.5, 34.9, 100, and 100% at 100, 150, 200, 250, and 300 °C. Therefore, we selected 250 °C as an optimum condition for 100% conversion. After 70 min, CO conversion decreased suddenly due to the CO poisoning on Pt site. Consequently, for use in long-term operation, this problem should be solved by using a bimetallic system or increasing the metal loading. In case of a bimetallic system, Ru as a promoter could oxidize CO to CO$_2$ by adsorbing OH which is more easily adsorbed on Ru than Pt. As Ru-Pt catalyst adsorbs OH in the atmosphere, CO oxidation rate increases more than Pt catalyst [17]. CO conversion was also affected by the Pt loading, as shown in Fig. 6. When Pt contents in alumina were adjusted from 0.5 to 1.5 wt%, CO conversions increased from 13 to 100%. In Pt loading, optimum activity was shown at 1.5 wt% Pt/Al$_2$O$_3$ catalysts. When we used 4 wt% Pt/Al$_2$O$_3$, stable reaction time could be extended to

Fig. 4. X-ray diffraction patterns of platinum and catalyst of (a) 0.5 wt% Pt/Al$_2$O$_3$, (b) 1.5 wt% Pt/Al$_2$O$_3$, (c) 2.5 wt% Pt/Al$_2$O$_3$ and (d) standard card data of platinum (JCPDS 4-802).

2. CO Oxidation

As-made Pt/Al$_2$O$_3$ catalysts were tested with several different reaction temperatures and compared with a commercial support.
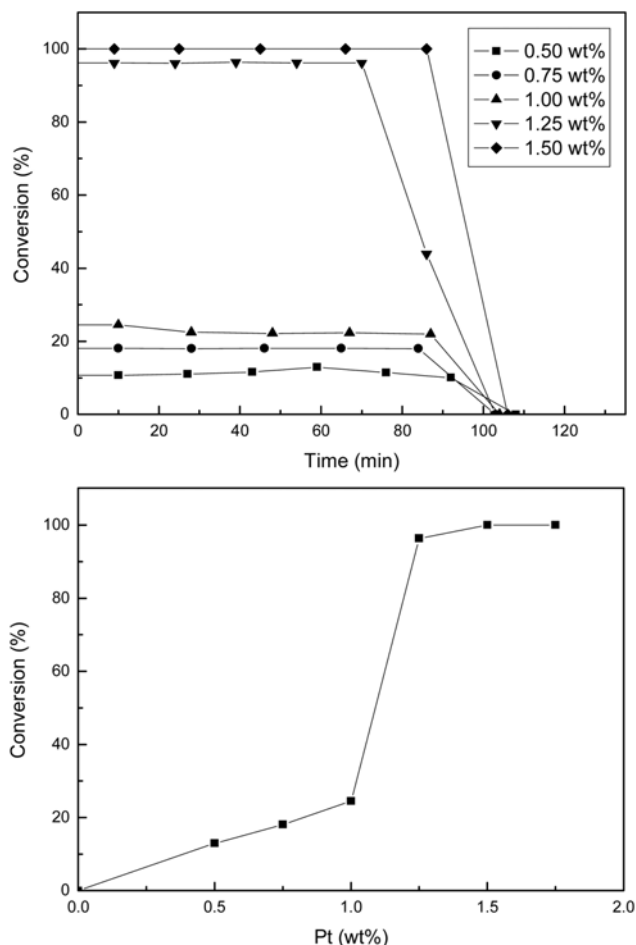
Fig. 6. CO conversion with Pt loading on nanoporous alumina.

above 20 min. These results suggested that in case of high Pt over 1.5 wt% in alumina, Pt could not be supported on the alumina, so it was free to move and also aggregate with each other or debased activity of catalysts by interrupting the alumina pore. Fig. 7 shows that stability of reaction was depending on the support structure at
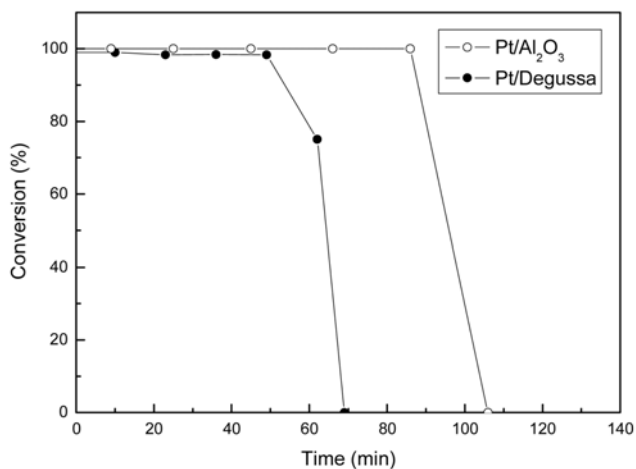

Fig. 7. Comparison of CO oxidation between nanoporous and Degussa catalysts (1.5 wt% and 250 °C).

the same condition (1.5 wt% Pt, 300 mg and 250 °C), such that the active zone of Degussa catalyst was smaller than nanoporous alumina. It seems to be compatible with surface area analysis that Degussa alumina had smaller surface area and pore structure, compared to nanoporous alumina. The converted CO_2 was easily removed by use of adsorbent, which has been reported elsewhere [15]. And then we can obtain pure H_2 from syngas.

CONCLUSIONS

To separate H_2 as alternative energy resource from syngas (CO, CO_2, and H_2), CO oxidation was performed using Pt/Al₂O₃ catalyst. Through this reaction, we made a tracing of pure hydrogen production process where CO generated from the gasification of waste was converted into CO_2 which could be easily removed. Nanoporous Pt/Al₂O₃ catalyst was prepared using precipitation method. Catalytic reactions were carried out for various reaction temperatures and content of Pt. Results in CO oxidation for various temperatures (100-300 °C) indicated that the highest conversion (100%) was obtained at above 250 °C with 1.5 wt% Pt/Al₂O₃. Nanoporous catalyst showed 40% longer reaction time, compared to Degussa catalyst. It might be due to larger active sites with smaller pore size and larger surface area than Degussa alumina.

ACKNOWLEDGEMENTS

REFERENCES

1. A. Baral and G. S. Guha, *Biomass Bioenergy*, **27**, 41 (2004).
2. A. Popovic, D. Djordjevic and P. Polic, *Environ. Int.*, **26**, 251 (2001).
3. M. Steinberg, *Int. J. Hydrogen Energy*, **24**, 771 (1999).
4. A. Thür, S. Furbo and L. J. Shah, *Sol. Energy*, **80**, 1463 (2006).
5. D. A. Bechrakis, E. J. McKeogh and P. D. Gallagher, *Energy Convers. Manage.*, **48**, 46 (2006).
6. C. Forsberg, *Prog. Nucl. Energy*, **47**, 484 (2005).
7. R. Edwards, D. Tsay and M. Hsu, *Fuel Cells Bull.*, **2004**, 10 (2004).
8. L. Zhou, Y. Guo, Q. Zhang, M. Yagi, J. Hatakeyama, H. Li, J. Chen, M. Sakurai and H. Kameyama, *Appl. Catal., A*, **347**, 200 (2008).
9. B.-T. Teng, J. Chang, J. Yang, G. Wang, C. Zhang, Y.-Y. Xu, H.-W. Xiang and Y.-W. Li, *Fuel*, **84**, 917 (2005).
10. K. Takehira, J. Shimomura, S. Hamakawa, T. Shishido, T. Kawabata and K. Takaki, *Appl. Catal., B*, **55**, 93 (2005).
11. Y. Cui, H. Zhang, H. Xu and W. Li, *Appl. Catal.*, **318**, 79 (2007).
12. S. Cavenati, C. A. Grande and A. E. Rodrigues, *Chem. Eng. Sci.*, **61**, 3893 (2006).
13. T. Moritz, S. Benfer, P. Arki and G. Tomandl, *Colloids Surf., A*, **195**, 25 (2001).
14. U. Heiz and U. Landman, *Nanocatalysis*, Springer (2006).
15. J.-S. Bae, J.-W. Park, J.-H. Kim, J.-G. Lee, Y. Kim and C. Han, *Korean Chem. Eng. Res.*, **47**, 646 (2009).
16. J.-K. Kim, Y. Kim, J.-W. Park, J.-S. Bae, D.-Y. Yoon, J.-G. Lee, J.-H. Kim and C. Han, *Korean J. Chem. Eng.*, **26**, 32 (2009).
17. H. Massong, H. Wang, G. Samjeské and H. Baltruschat, *Electrochim. Acta*, **46**, 701 (2001).